N63-14714

Code 1

23p.

NASA TN D-1687

NASA TN D-1687

TECHNICAL NOTE

D-1687

THE ARTIFICIAL RADIATION BELT MADE ON JULY 9, 1962

Wilmot N. Hess

Goddard Space Flight Center
Greenbelt, Maryland

NATIONAL AERONAUTICS AND SPACE ADMINISTRATION

WASHINGTON April 1963

copy 2

Code 1

THE ARTIFICIAL RADIATION BELT MADE ON JULY 9, 1962

by
Wilmot N. Hess
Goddard Space Flight Center

SUMMARY

The available information on the artificial radiation belt formed by the July 9, 1962, high altitude nuclear explosion is reviewed. Data from Injun (1961 o2), Telstar I (1962 $\alpha\epsilon$1), Traac (1961 $\alpha\eta$2), and Ariel I (1962 o1) are combined to form one picture of the artificial belt. The data are consistent to about a factor of 3. The flux map obtained in this way is used to calculate the flux encountered by several satellites. These show reasonable agreement with data on solar cell damage. Preliminary data on particle lifetimes are presented. Particles at $L > 1.30$ are expected to last several years on the basis of coulomb scattering. Crude calculations of shielding are made to indicate the doses received inside various vehicles.

CONTENTS

Summary i

INTRODUCTION 1

AVAILABLE DATA 1

ANALYSIS OF THE DATA 2

FLUX PLOTS 4

VEHICLE-ENCOUNTERED FLUXES 12

MANNED FLIGHT 17

PARTICLE TIME HISTORIES 17

References 18

Appendix A—Shielding and Radiation Doses 19

THE ARTIFICIAL RADIATION BELT MADE ON JULY 9, 1962*

by

Wilmot N. Hess

Goddard Space Flight Center

INTRODUCTION

On July 9, 1962, at 0900:09 UT a nuclear explosion of about 1.4 megatons was carried out at 400 kilometers above Johnston Island in the Pacific Ocean. This explosion produced, as was expected, an artificial radiation belt. However, the intensities in this radiation belt are considerably higher than were expected. Three days after the explosion the U.S.-U.K. joint satellite Ariel I (1962 o1) stopped transmitting. On August 2, Transit IV-B (1961 $\alpha\eta$1) stopped transmitting; Traac (1961 $\alpha\eta$2) stopped on August 14. Instruments on Ariel I, Traac, and Injun (1961 o2) showed large particle fluxes shortly after the explosion. It took about a month to start getting some grasp of the characteristics of the new radiation belt. This is a status report on the new belt as of September 12.

AVAILABLE DATA

The information that is available to form a picture of the new radiation belt comes mostly from particle detectors on the Ariel I, Injun, Traac, and Telstar I (1962 $\alpha\epsilon$1) satellites. In addition to these data we can use the observed solar cell damage on satellites as an integral measurement of the trapped electron flux. Also, some data are available from dosimetry measurements.

Some of the original data about the enhanced trapped particle fluxes after the July 9 explosion came from the x-ray detector on the Ariel I satellite (private communication from A. Willmore, University College, London). This instrument was not designed to count charged particles and therefore its efficiency is uncertain. The data from it are quite useful in studying the time decay of the trapped flux and in locating contours of constant flux in B-L space.

Data received by the shielded 213 GM counter on Injun have been analyzed to give the first picture of the new radiation belt (Reference 1). This counter is the background channel of the magnetic spectrometer, SpB. It has 3-1/2 gm/cm^2 of Pb shielding and about 1 gm/cm^2 of wall and miscellaneous shielding. It was supposed to give the penetrating background to be subtracted from the other channels

*This is an abridged version of Technical Memorandum X-788, a confidential report entitled "The Artificial Radiation Belt." This version will also be published in the *Journal of Geophysical Research*.

of the spectrometer. This detector is now called on to provide quantitative information, and it has been calibrated after the fact. It is nearly omnidirectional. Fluxes are obtained from the count rates by dividing by $G_o = 0.11\ cm^2$. Other detectors on Injun also give useful data sometimes, but often they are saturated and not usable. So far, little data have been analyzed from any Injun detectors except SpB.

Telstar I has on it a solid state p-n junction detector with pulse height analysis that selects electrons in different energy ranges from 0.2 to 1 Mev (private communication from W. Brown, Bell Telephone Laboratories). A lot of data have been reduced from Telstar I for two channels of the electron detector. This detector has given all the data currently available at high altitudes. It is directional, with an aperture half-angle of about 10 degrees. The fluxes are made omnidirectional by multiplying by the appropriate solid angle factor and then using a factor between 1 and 2 to correct, roughly, for the nonisotropic angular distribution.

Traac has a 302 GM counter shielded by $0.265\ gm/cm^2$ of Mg, which will count electrons of energy above 1.5 Mev (private communication from G. Pieper and L. Frank, Applied Physics Laboratory). It is essentially omnidirectional. Fluxes are obtained by dividing by $G_o = 0.75\ cm^2$ and correcting for saturation for high count rates.

ANALYSIS OF THE DATA

The data from these four satellites must be combined to form one overall picture of the artificial radiation belt. To do this assume that the energy spectrum of the electrons being counted is a fission spectrum. This is certainly the best guess. We will compare the data on this basis and see if there is agreement in the regions where direct comparison is possible. The fission energy spectrum N(E) is shown in Figure 1, curve A. A calibration of the Telstar I detectors at the Los Alamos Scientific Laboratory in a fission electron beam gives f, the fraction of fission electrons counted by the detectors, equal to 1/2.8 for the 240-340 kev channel and 1/6.0 for the 440-680 kev channel.

For Injun we have the experimentally determined factor 1/f of several thousand, by comparison of two detectors on board. The 213 GM counter has also been calibrated at Los Alamos with a fission electron spectrum (private communication from A. Petschek, H. Motz, and R. Taschek, Los Alamos Scientific Laboratory), and the factor f determined this way is 1/4000. We will use this factor in the present analysis. The Los Alamos tests show that the detector counts bremsstrahlung from electrons of several Mev rather than direct penetrating electrons. (If the shield had been carbon rather than lead, the counter would have counted direct penetrating electrons.)

For Traac, f is determined by considering the penetration of electrons through the detector shield of $0.265\ gm/cm^2$ of Mg and through the wall of $0.400\ gm/cm^2$ of stainless steel. Using the range straggling data (Reference 2) for Al we can get the fraction of electrons that penetrate a shield of given thickness, as shown in Figure 2. The expression for the extrapolated range R is

$$R = 0.526E - 0.094 .$$

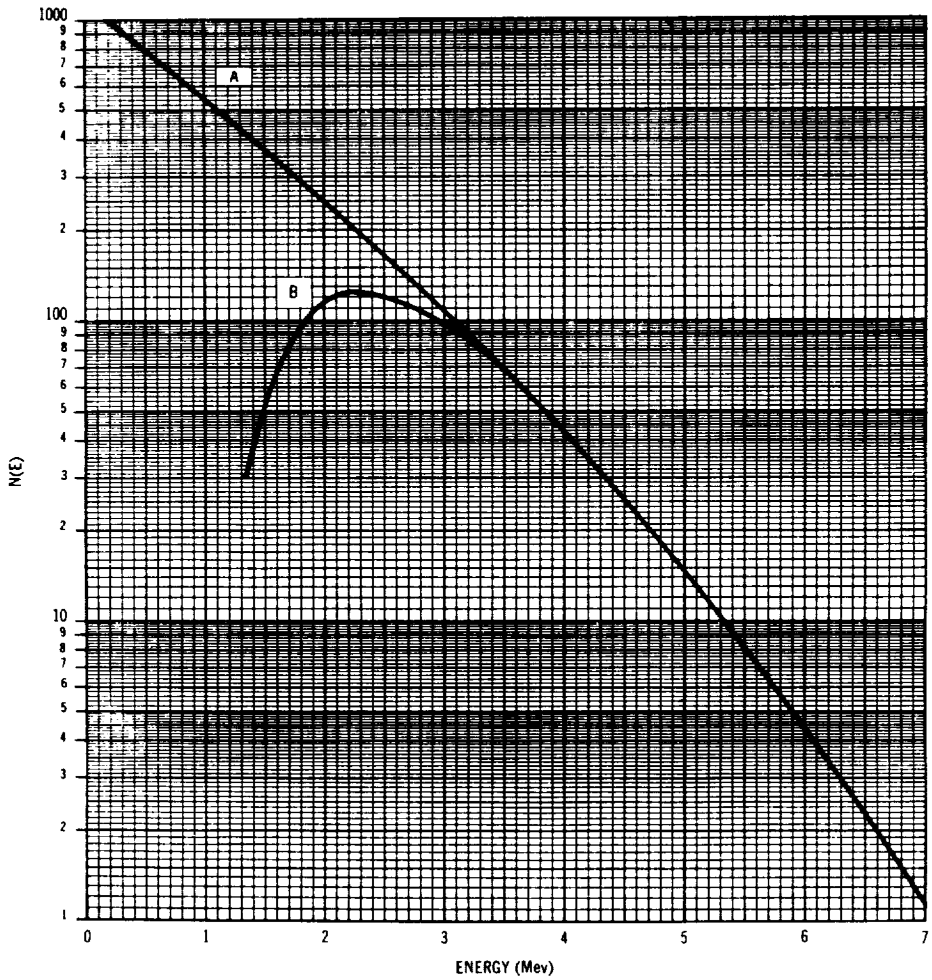

Figure 1—Curve A is the fission energy spectrum and curve B the transmission energy spectrum for the Traac GM counter (0.66 gm/cm² wall).

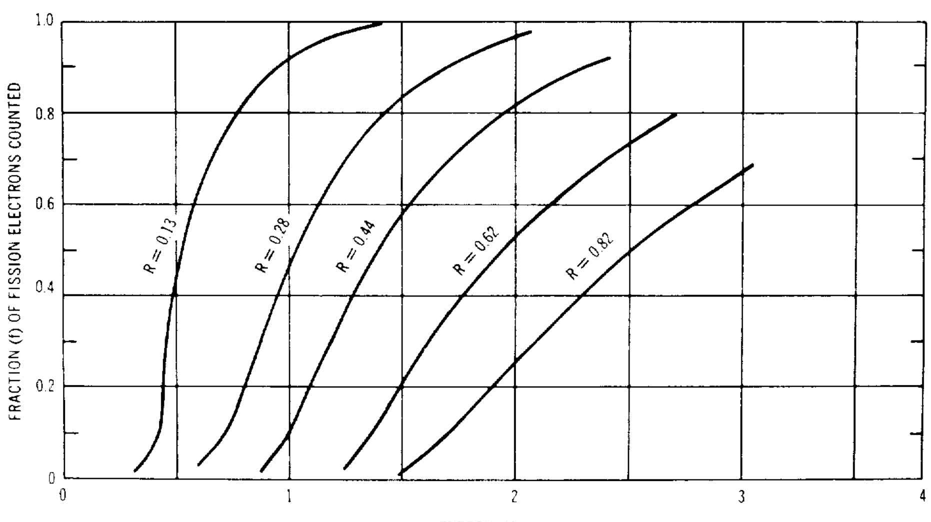

Figure 2—The fraction of electrons of different energies that penetrate different shield thicknesses of Al.

This yields the absorber thickness that gives 10 percent transmission for electrons of energy E. For 50 percent transmission we multiply the energy by 1.38, and for 80 percent transmission increase the energy by a factor of 1.92. In this way we get the electron transmission spectrum, curve B in Figure 1. The energies of the transmitted electrons are different from curve B, but the number transmitted is given correctly. The integral under this curve gives f = 1/5.5 for the Traac counter. More information on shielding calculations is given in Appendix A.

Using the factors for the several detectors, we can calculate the total flux of fission electrons. In order to compare the different detectors, the total flux along several field lines (actually narrow ranges of L) has been plotted for different values of B (Figure 3). These plots show that the different detectors agree fairly well in flux values. Avoiding the first day after the nuclear explosion (labeled by the number 0 inside the symbols on the graphs) we can see quite smooth trends in the data. The flux from Telstar I may be as much as twice as high as Injun fluxes. Traac and Injun agree quite well where comparisons are possible. In general, the data shows agreement to a factor of 2.

This agreement of the data shows two things: First, because the detectors give internally consistent results it seems likely that all the detectors are giving accurate information. Secondly, the assumption that the electrons have a fission energy spectrum appears to be correct. Of course it is possible that the energy spectrum is not a fission spectrum and also that the detectors are not in agreement, but it would have to be a peculiar combination of such effects that would give the agreement shown here. A comparison of the four channels of the Telstar I electron detector also indicates that the energy spectrum is fission-like up past 1 Mev.

FLUX PLOTS

Now that it has been demonstrated that the energy spectrum is essentially a fission spectrum at least in the region of data overlap we can use all the counter data to construct a composite flux map in B-L space. As McIlwain has shown, these magnetic coordinates are the best way of organizing data about trapped particles (Reference 3). L is constant along a field line in space and, for a dipole, is the distance from the center of the earth to the equatorial crossing of the line, in units of earth radii (Figure 4). Values of L are calculated from the real values of the earth's field.

In constructing the flux map for $B > 0.15$ gauss and for $L < 2.0$ earth radii the graphs in Figure 3 are used to locate the flux contours. The experimental data outside this B-L region are essentially all from Telstar I. There are several weeks data from Telstar I and considerable redundancy. The map made this way is quite complete. The data available in early September gave the flux map in Figure 5. This map is for about 1 week after the explosion. There was considerably more flux at low altitudes at early times.

This same data plotted in R-λ coordinates, where

$$B = \frac{M}{R^3} \sqrt{4 - \frac{3R}{L}} ,$$

$$R = L \cos^2 \lambda ,$$

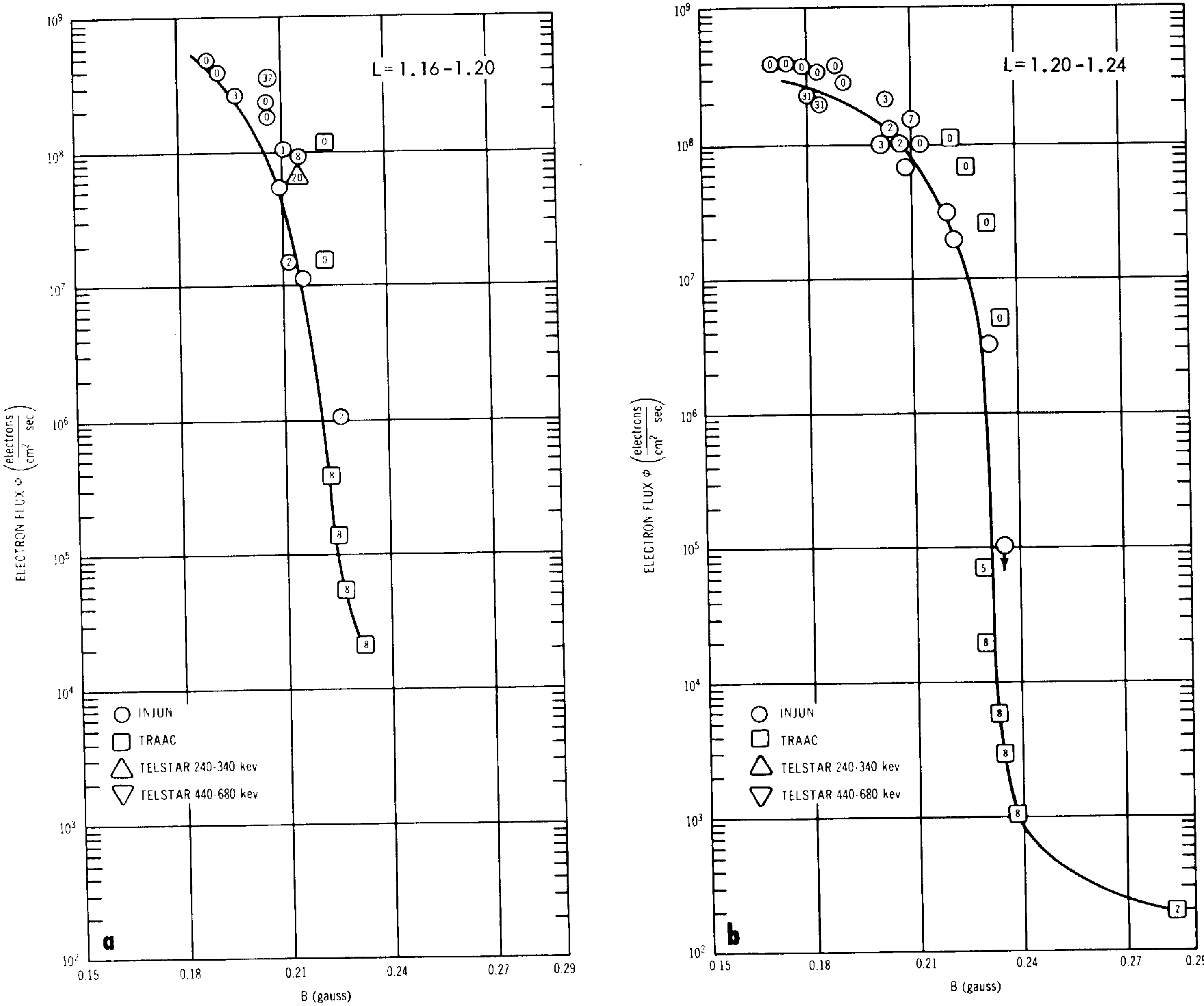

Figure 3—The electron flux distributions along different field lines.

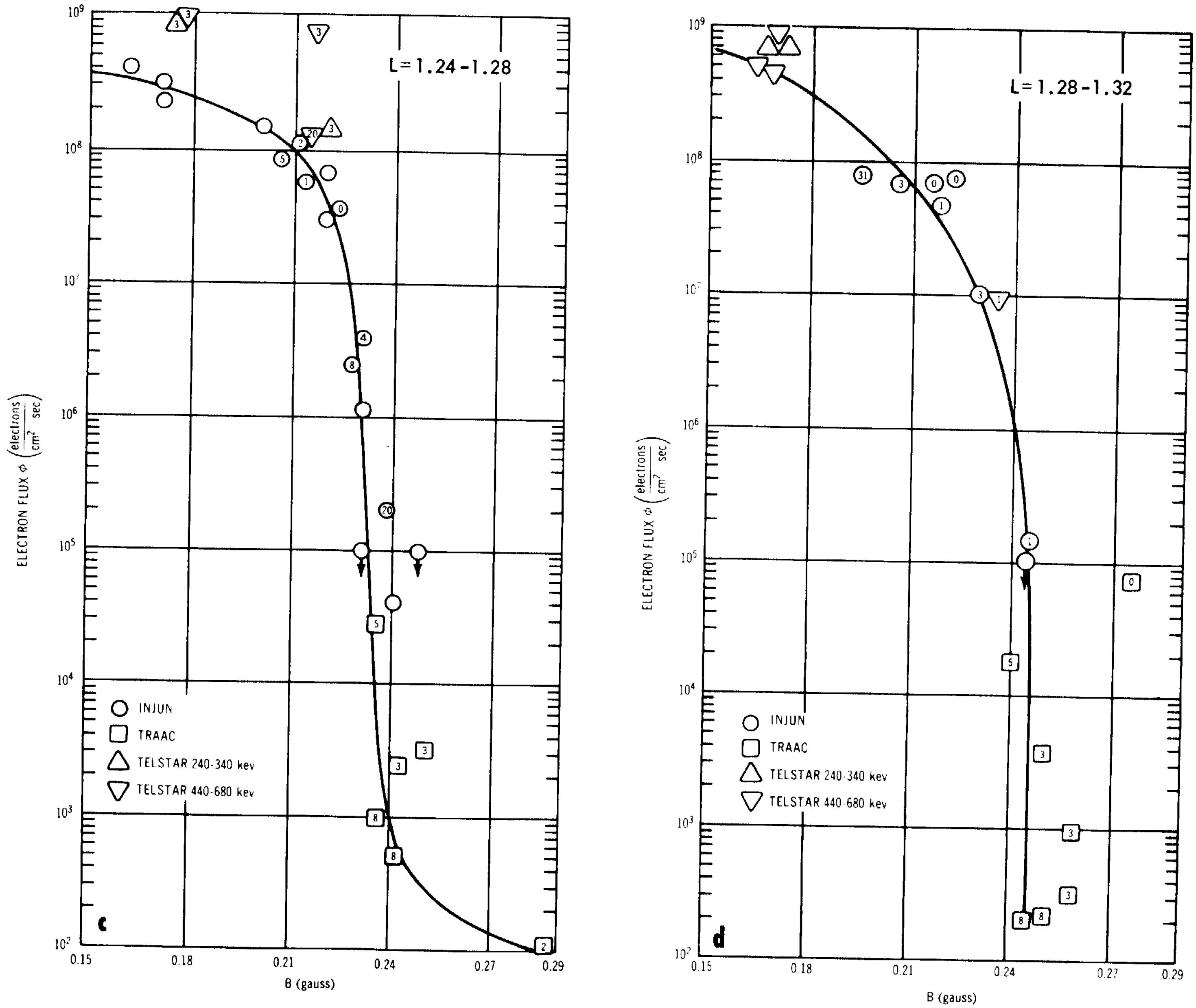

Figure 3 (continued)—The electron flux distributions along different field lines.

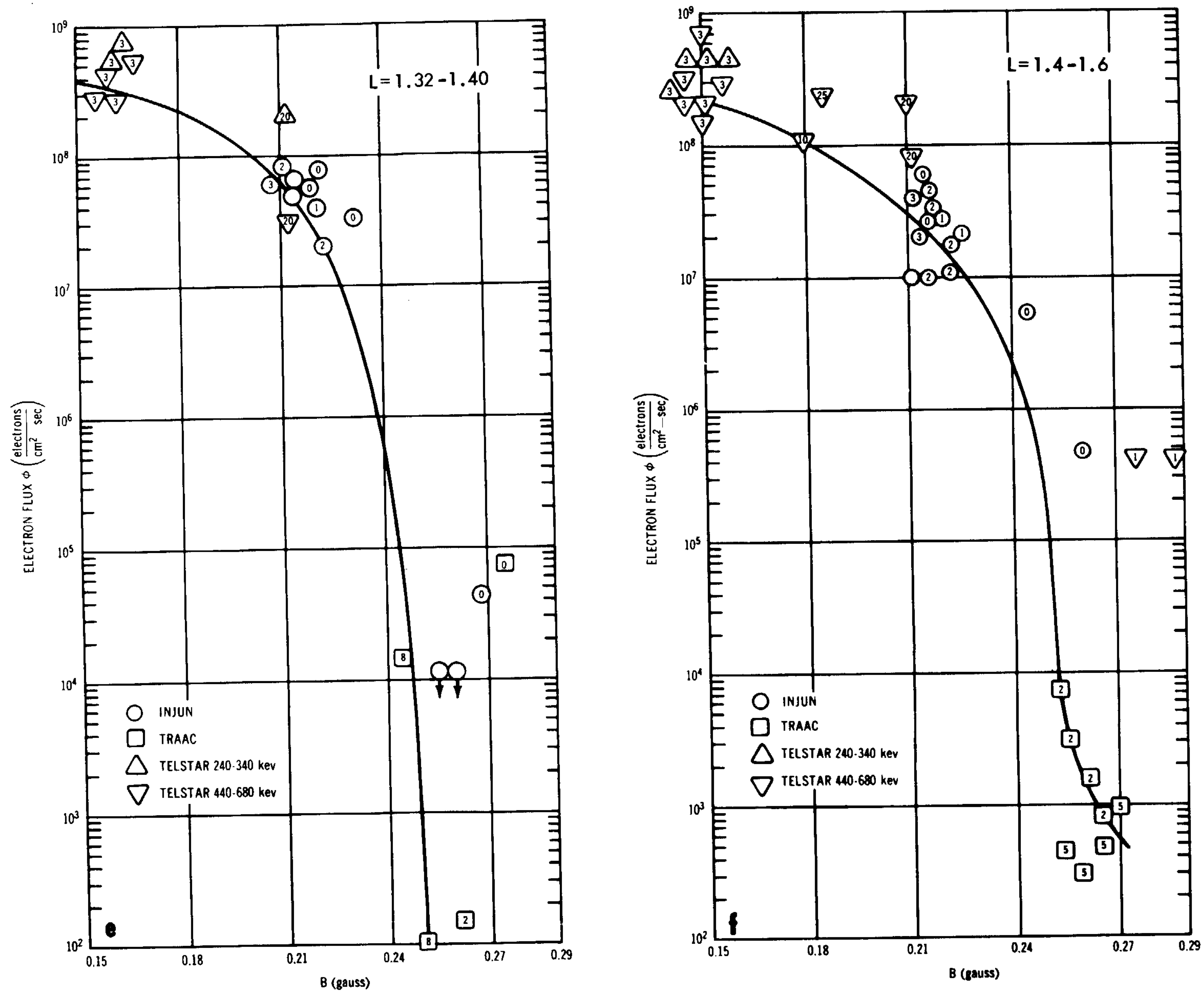

Figure 3 (continued)—The electron flux distributions along different field lines.

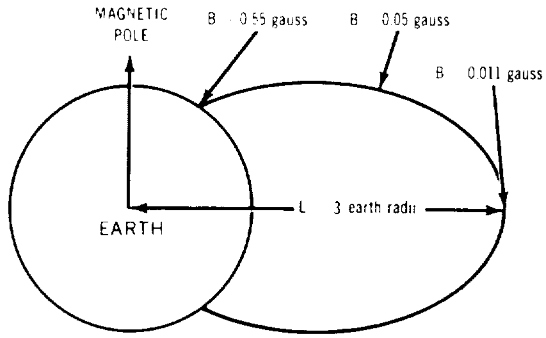

Figure 4—The B-L magnetic coordinate system.

gives an equivalent dipole representation of the earth's field (Figure 6). The maximum electron flux is about 2×10^9 elec/cm^2-sec. Integrating to get the total number of electrons stored in the field we find

$$\int \phi \, dV = 2 \times 10^{26} \text{ electrons.}$$

About 40 percent of these electrons lie inside the 10^9 contour and about 60 percent of these electrons lie inside the 3×10^8 contour. It is not certain what fraction of these electrons are bomb-induced and what fraction are natural electrons. In this region around $L < 1.5$ the energy spectrum seems softer than a fission spectrum.

The B-L flux map when plotted in terms of geographic coordinates gives the flux contours for different altitudes shown in Figure 7.

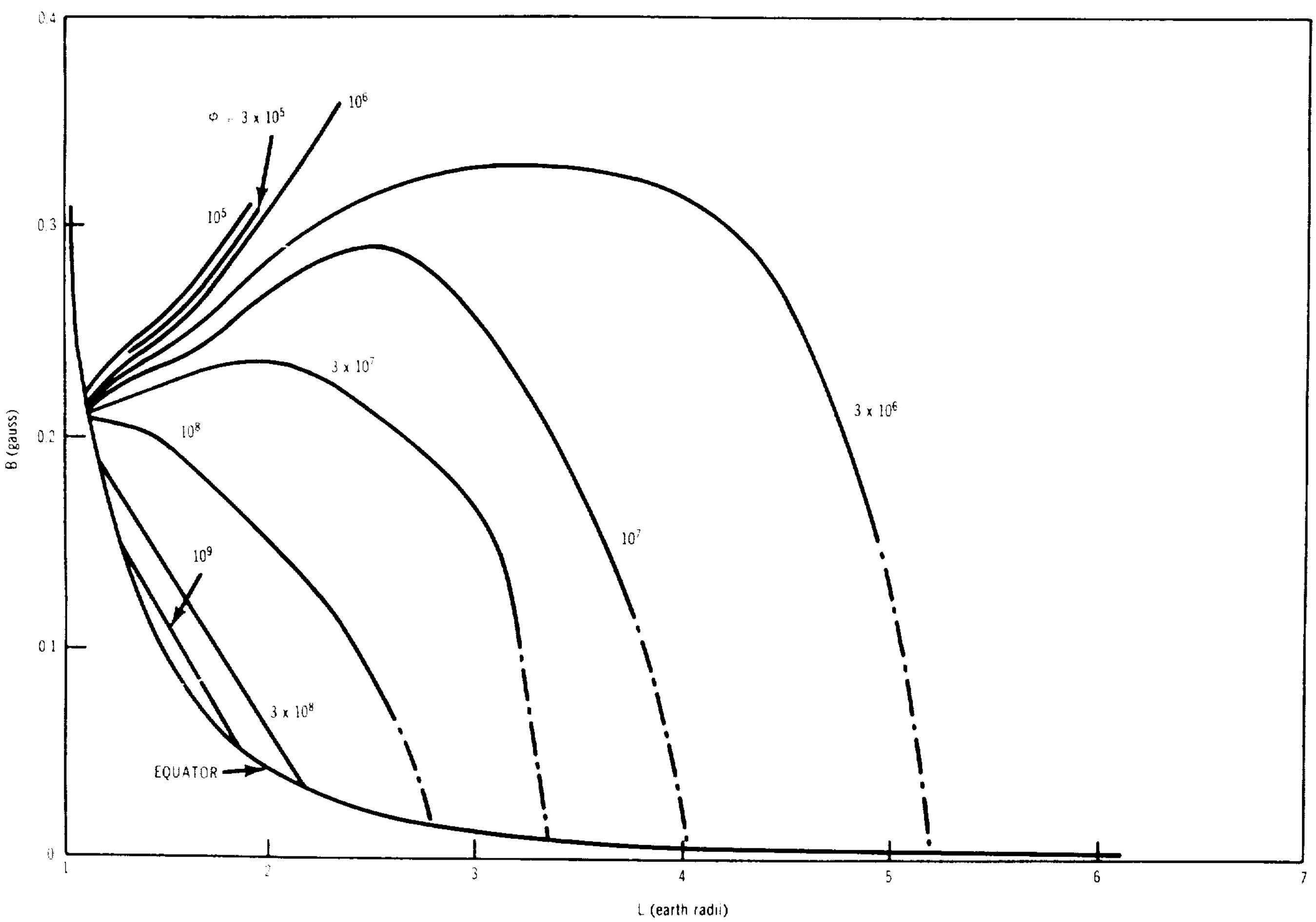

Figure 5—The B-L map of electron fluxes.

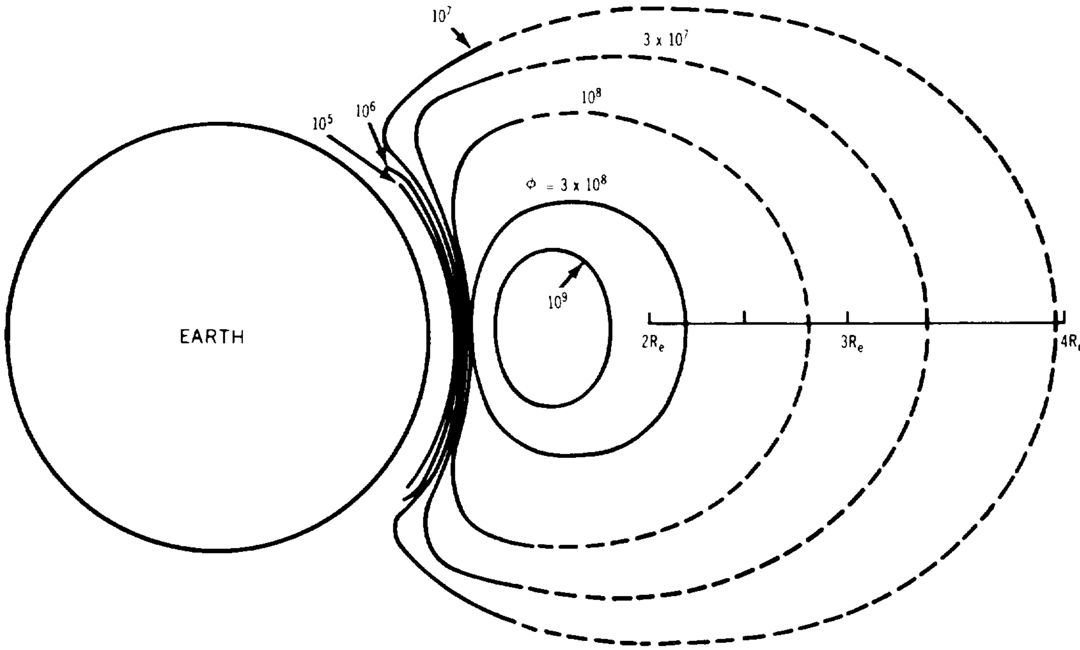

Figure 6—The R-λ map of electron fluxes (an ideal dipole representation of the earth's field).

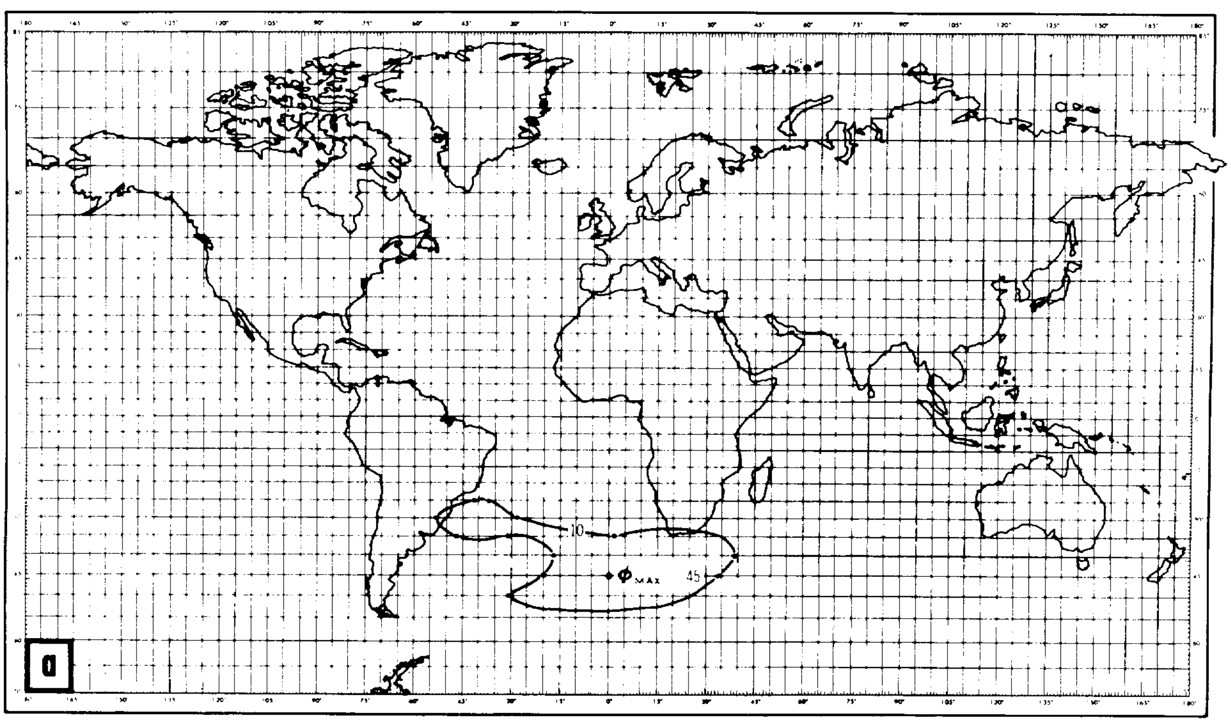

AT 200 km

Figure 7—Electron flux maps at different altitudes above the earth's surface. Flux is in units of 10^5 electrons/cm^2-sec.

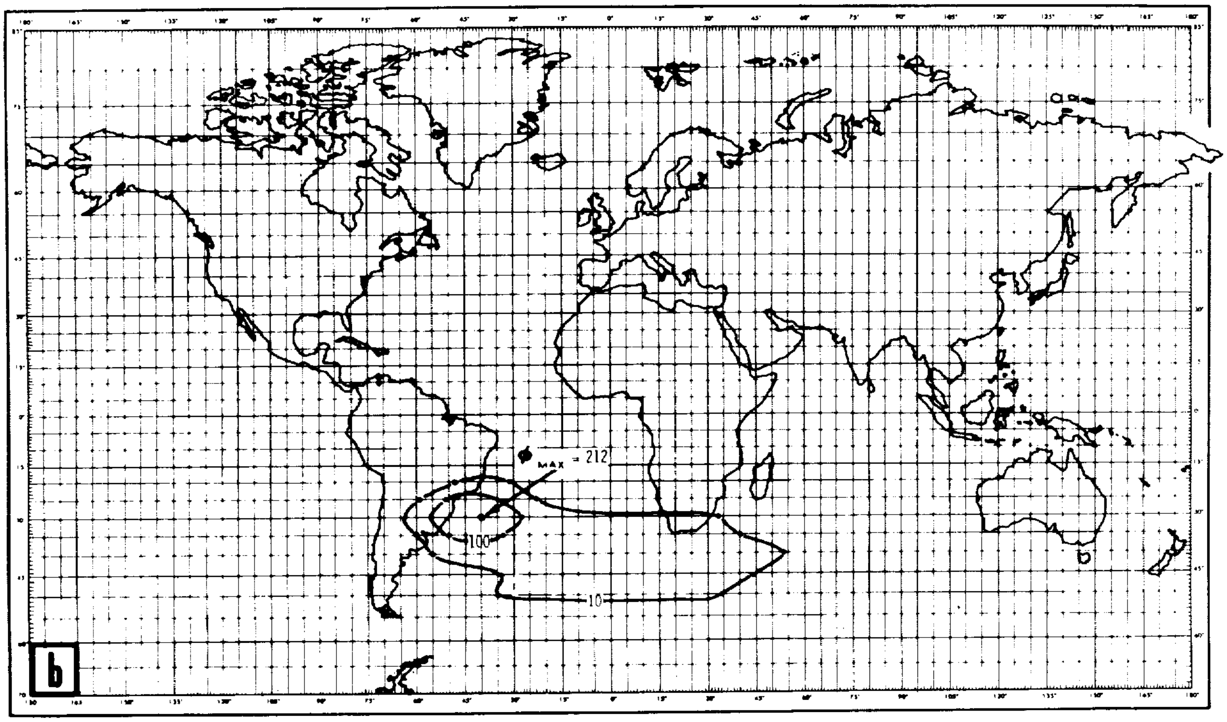

AT 300 km

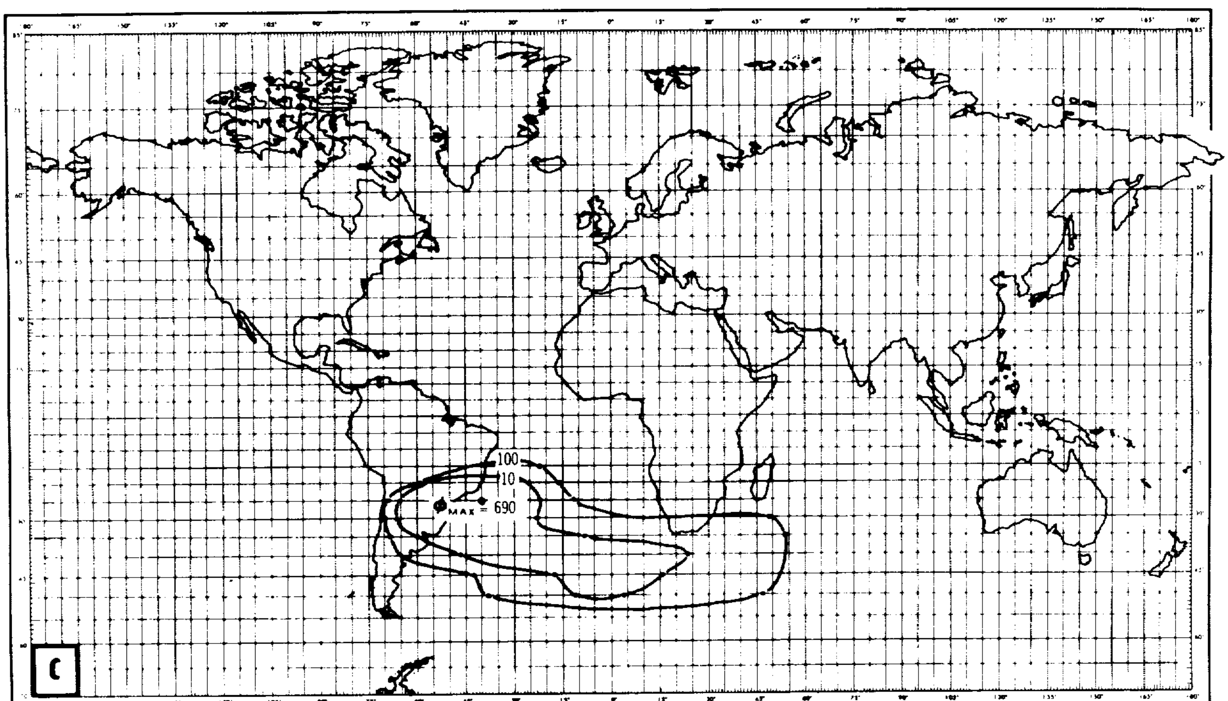

AT 400 km

Figure 7 (continued)—Electron flux maps at different altitudes above the earth's surface. Flux is in units of 10^5 electrons/cm^2-sec.

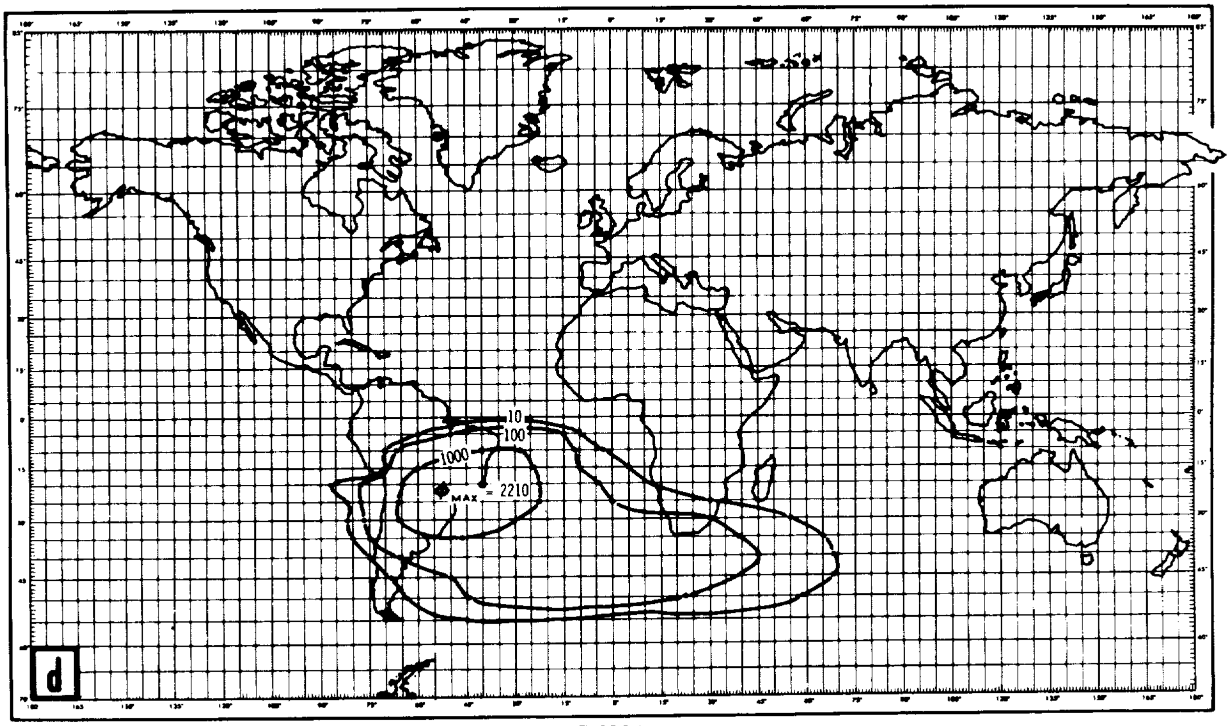

AT 600 km

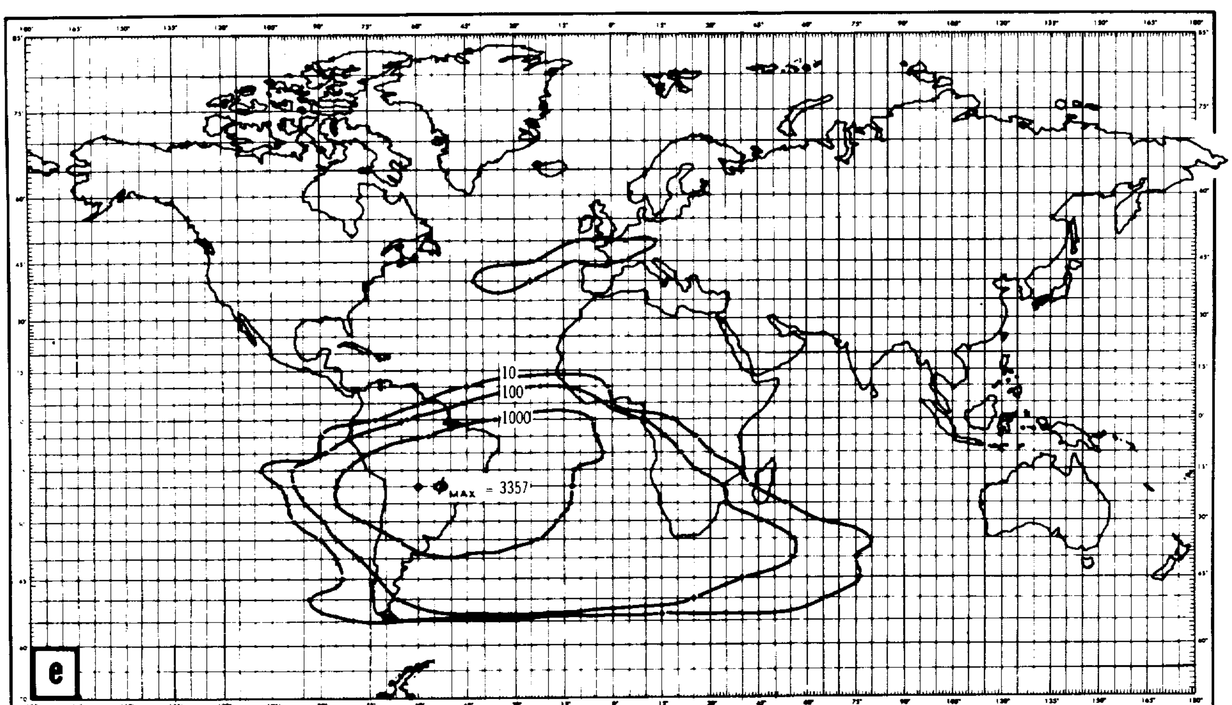

AT 800 km

Figure 7 (continued)—Electron flux maps at different altitudes above the earth's surface. Flux is in units of 10^5 electrons/cm^2–sec.

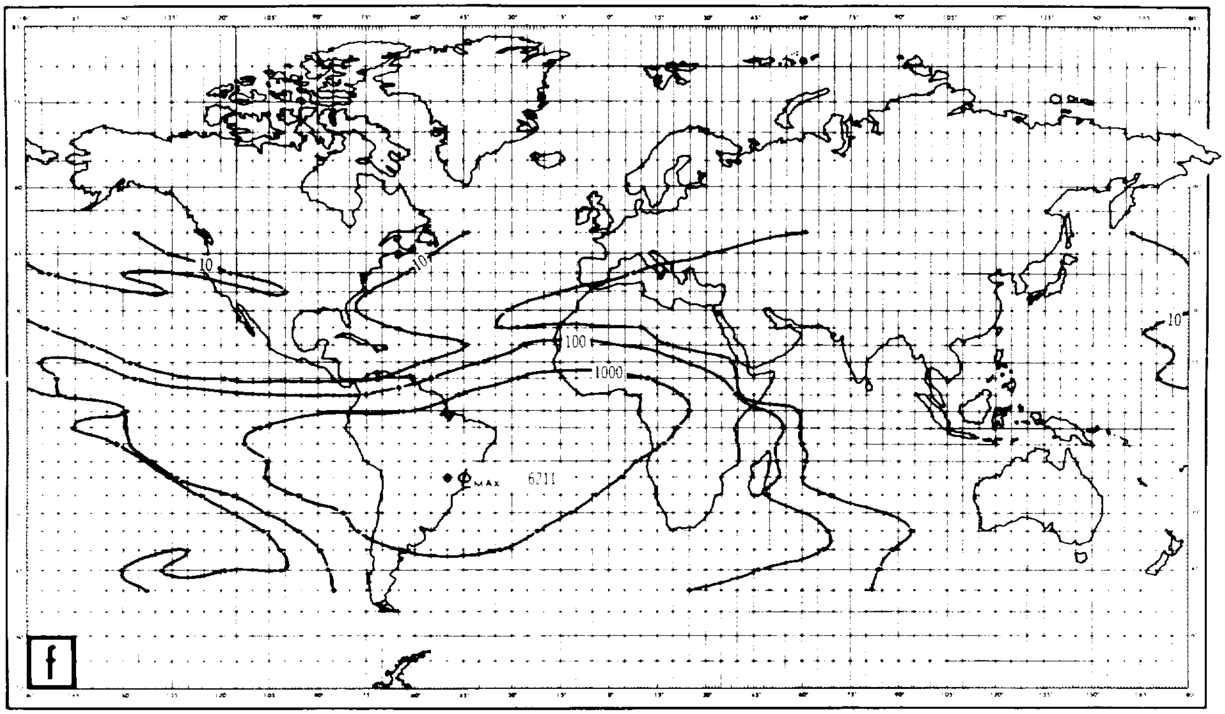

AT 1000 km

Figure 7 (continued)—Electron flux maps at different altitudes above the earth's surface. Flux is in units of 10^5 electrons/cm^2-sec.

VEHICLE-ENCOUNTERED FLUXES

A machine code has been developed which calculates the total number of electrons/cm^2 in the artificial radiation belt that strike a vehicle in space. This is done by calculating a point on the vehicle trajectory, transforming to B-L coordinates, looking up the electron flux, and integrating along the vehicle orbit. This has been performed and the encountered fluxes have been determined for all of the vehicles listed in Table 1. These fluxes have been transformed into r/day by using 3×10^7 electrons/cm^2 = 1 r. The orbital elements of these vehicle trajectories are given in Table 2.

From the encountered fluxes in Table 1, we can learn several things. Let us first consider solar cell damage. The Bell Telephone Laboratories staff have studied this problem in considerable detail and prepared Figure 8, which shows how different type cells are damaged by 1 Mev electron irradiation (Reference 4 and private communication from the authors of that paper). Above about 0.5 Mev the electron damage is essentially independent of energy. Some care must be exercised in using this chart because of the variation in the characteristics of solar cells. We will assume all the electrons in the flux spectrum in Figure 5 are greater than 0.5 Mev in estimating the solar cell damage.

About 20 percent degradation was needed by the blue sensitive p-on-n type cells on Ariel I to produce the observed power supply damage (private communication from A. Franta, Goddard Space

Table 1

Calculations on Fluxes Encountered by Satellites Moving Through the Artificial Radiation Belt.

Datum	Ariel I	Traac and Transit IV-B	Telstar I	Tiros V	Orbiting Solar Observatory I (1962 ζ1)	Relay*	Polar Orbiting Geophysical Observatory (Pogo)*
Perigee (km)	390	960	952	590	552	1343	257
Apogee (km)	1210	1106	5660	971	594	5555	931
Inclination (degrees)	54	32	45	58	33	50	90
Altitude (km) at 30° S Lat 30° W Long	1067	1000	5138 1758	963	594	4371 1516	804
Calculated r/day Outside Vehicle	110,000	180,000	800,000	46,000	27,000	1.1×10^{6}	22,000
Code Output from Machine	$\frac{3.1 \times 10^{9}}{4}$	$\frac{5.0 \times 10^{9}}{4}$	$\frac{2.2 \times 10^{10}}{4}$	$\frac{1.28 \times 10^{9}}{4}$	$\frac{7.5 \times 10^{8}}{4}$	$\frac{3.0 \times 10^{10}}{4}$	$\frac{6.2 \times 10^{8}}{4}$
Length of Machine Run in Satellite Days	4	4	4	4	4	4	4
Electrons/cm^2-day	2.8×10^{12}	4.5×10^{12}	2.0×10^{13}	1.15×10^{12}	6.8×10^{11}	2.7×10^{13}	5.6×10^{11}
Protons/cm^2-day	—	—	—	—	—	—	—

*To be launched.

Table 1 (continued)

Calculations on Fluxes Encountered by Satellites Moving Through the Artificial Radiation Belt.

Datum	1000 km Polar Orbit†	800 km Polar Orbit	Orbiting Astronomical Observatory*	SERB*	MA-7 (1962 τ1)
Perigee (km)	1000	800	802	278	160
Apogee (km)	1000	800	817	16,668	264
Inclination (degrees)	90	90	31	17.0	33
Altitude (km) at 30° S Lat 30° W Long	1000	755	810	—	261
Calculated r/day Outside Vehicle	80,000	27,000	—	—	80‡
Code Output from Machine	$\frac{2.2 \times 10^9}{4}$	$\frac{1.04 \times 10^9}{4}$	$\frac{2.2 \times 10^9}{4}$	$\frac{1.4 \times 10^{10}}{4}$	3.45×10^6
Length of Machine Run in Satellite Days	4	4	4	4	0.4 (9.5 hours)
Electrons/cm^2-day	2×10^{12}	9×10^{11}	2×10^{12}	1.2×10^{13}	0.24×10^{10} ‡
Protons/cm^2-day	—	—	—	—	—

*To be launched.

†Similar to Nimbus, the Fixed Frequency Topside Sounder, the Swept Frequency Topside Sounder, and the Polar Ionosphere Beacon (which have been or will be launched).

‡Six orbits only.

Table 2

Orbital Elements of Various Space Vehicles.

Element	Ariel I	Traac and Transit IV-B	Telstar I	Tiros V	OSO I	Relay
Epoch (days, hours, min, sec)	190, 9, 0, 0	190, 4, 3, 46.506	191, 8, 51, 0	190, 9, 0, 0	190, 9, 0, 0	305, 0, 0, 0
Semimajor Axis (earth radii)	1.1254	1.1618	1.5182	1.1224	1.0900	1.5407
Eccentricity	0.05714	0.009922	0.2430	0.02663	0.003012	0.2143
Inclination (degrees)	53.866	32.423	44.803	58.102	32.855	50.0003
Right Ascension of Ascending Node (degrees)	-24.881	96.434	-156.222	-75.536	154.502	163.708
Argument of Perigee (degrees)	-9.2537	-51.6890	164.811	118.014	139.136	-167.526
Mean Anomaly (degrees)	-86.8833	0.0001	1.1684	-194.11968	-164.5453	7.8219

Table 2 (continued)

Element	Pogo	1000 km Polar Orbit	MA-7	800 km Polar Orbit	OAO	SERB
Epoch (days, hours, min, sec)	82, 3, 55, 32.101	190, 9, 0, 0	268, 14, 0, 0	190, 9, 0, 0	153, 0, 0, 0	303, 10, 0, 0
Semimajor Axis (earth radii)	1.0931	1.1568	1.0331	1.1254	1.1270	2.3284
Eccentricity	0.04830	0.1490×10^{-7}	0.008552	4.4703×10^{-7}	0.001074	0.5518
Inclination (degrees)	90.001	90.000	32.546	90	30.982	17.0
Right Ascension of Ascending Node (degrees)	-73.806	-158.175	75.069	-158.175	38.6643	17.2908
Argument of Perigee (degrees)	-19.408	-180.000	78.188	-180.000	-68.8243	134.6735
Mean Anomaly (degrees)	2.1956	0.0000	7.6908	0	36.7572	0

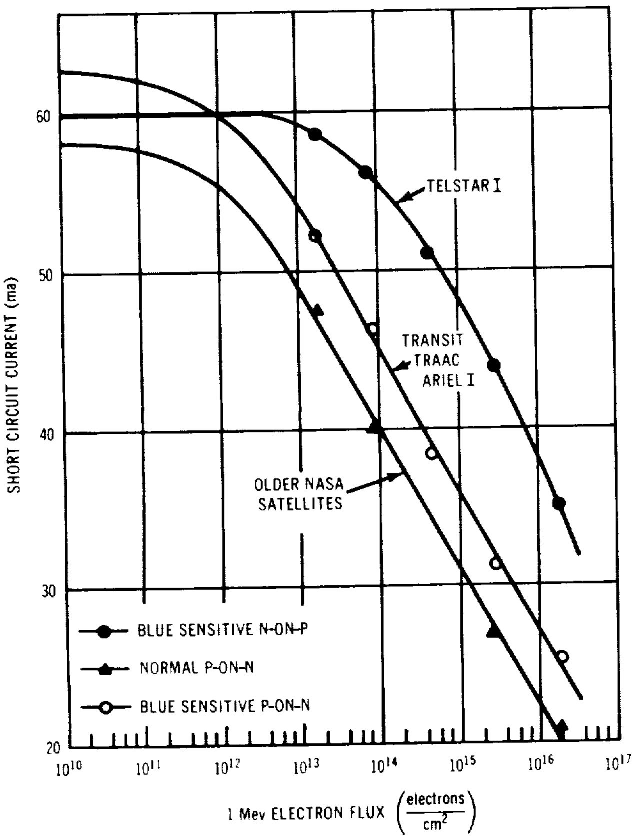

Figure 8—Solar cell damage curves.

Flight Center). This would be caused by about 10^{13} electrons/cm^2 according to Figure 8. About seven days after the nuclear explosion, this flux would have been achieved (Table 1 gives 2.8×10^{12} electrons/cm^2-day for Ariel I, of which half hit the face of the cells). The Ariel I power supply started malfunctioning in 3-1/2 days. This is quite good agreement.

Traac and Transit IV-B also had blue sensitive p-on-n solar cells, but it would take 3×10^{14} electrons/cm^2 to cause malfunction, because the cells were lower feficiency cells (private communication from R. Fischell, Applied Physics Laboratory). Table 1 gives 4.5×10^{12} electrons/cm^2 encountered per day. Half of these electrons hit the face of the cells. Traac stopped transmitting in 36 days and Transit IV-B in 24 days. Using 30 days as the average, we get a total encountered flux of 0.7×10^{14} electrons/cm^2, only in fair agreement with that required to produce damage.

Telstar I used the much more damage resistant n-on-p cells, because it was to routinely fly through the inner radiation belt protons. Even with the artificial radiation belt, its power supply lifetime is expected to be considerably longer than 1 year.

The Telstar I solar cells are degrading at a rate that would be produced by 6×10^{12} electrons/cm^2-day of 1 Mev hitting the bare cells (private communication from W. Brown, Bell Telephone Laboratories). This corresponds to about 1.8×10^{13} electrons/cm^2-day incident on the outside of the 30 mil sapphire covers. Our calculations give $1/2 \times 2 \times 10^{13} = 1 \times 10^{13}$ electrons/cm^2-day hitting the cells. The observed solar cell degradation on Telstar I should be somewhat more than that calculated from the artificial electron belt, because slow proton damage probably contributes somewhat to the degradation (private communication from W. Brown, Bell Telephone Laboratories).

We have neglected the enhanced early time effects here on all the exposed satellites. An appreciable part of the encountered flux may have been encountered in the first few days. For the first week after the explosion the flux was higher than that given in Figures 5 and 6.

Injun, Tiros V, and other satellites continue to function. Injun has a low duty cycle and Tiros V shows some solar cell degradation. Film badge dosimeter measurements have been made on several space flights. About 10 r/day was measured inside 1.5 gm/cm^2 of shielding. In order to compare this radiation dose with the predictions in Table 1, correction must be made for shielding. To do this we perform a calculation like that done for the Traac GM counter to get f, the fraction of electrons that penetrate the wall. Values of f have been calculated for different thicknesses of shield by using the relationship $R = 0.526E - 0.094$ and the associated rough-straggling transmission curves in Figure 3. Figure 9 shows a plot of 1/f as a function of shield thickness. This is really only true for Al but for lack of better information we will use it for other materials too. For 1.5 gm/cm^2 we get f = 1/50 for normal incidence particles. To correct for a distribution of incidence angles we will say roughly that about half as many get through. Also, 2π steradians are covered by a much thicker shield so that the total factor f' = 1/200. This would mean that 10 r/day × 200 = 2000 r/day were incident on the outside of the vehicle. This agrees to within a factor of 2 with the calculated vehicle-encountered flux.

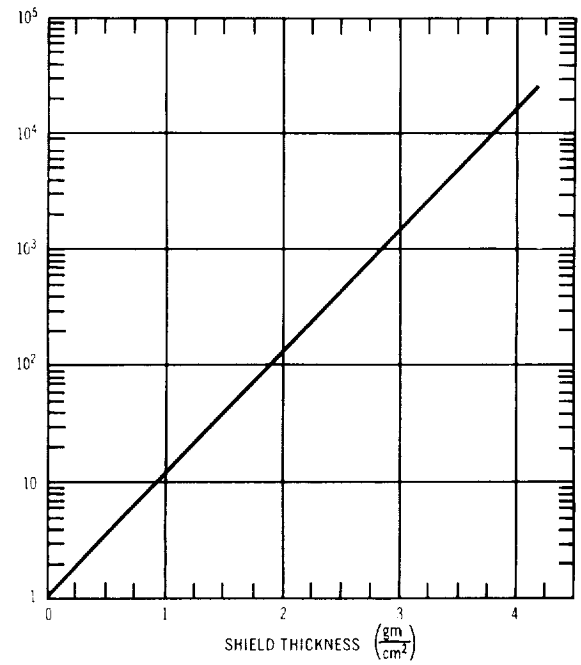

Figure 9—The fraction of fission electrons that penetrate different shield thicknesses.

MANNED FLIGHT

For a Mercury capsule orbit with an apogee of 264 km the total flux encountered in six orbits would be 0.24×10^{10} electrons/cm^2 outside the vehicle (Table 3). If the apogee is lowered by 30 km (to 234 km) the total flux for 6 orbits is reduced to 0.17×10^{10} electrons/cm^2. If the apogee is raised by 30 km (to 294 km) the total flux for 6 orbits is increased to 0.45×10^{10} electrons/cm^2.

PARTICLE TIME HISTORIES

Table 3

Flux per Orbit for a Mercury Capsule at an Altitude of 264 km.

Orbit	Flux (electrons/cm^2)
1	5.0×10^6
2	2.1×10^7
3	4.8×10^7
4	2.9×10^8
5	6.4×10^8
6	1.4×10^9

One of the important problems to answer about the new belt is how long it will last. The currently intense regions will last a number of years, according to present indications. At low altitudes the fluxes have already decayed a lot. According to Ariel I and Traac data, outside the 10^5 contour of the B-L plot in Figure 6 the fluxes decayed several orders of magnitude in a few days.

Injun has noted some decay at 1000 km (private communication from B. O'Brien, State University of Iowa). At L = 1.18 and B = 0.191 there is a decay factor of about 2 from +10 to +1000 hr.

For the same L and time interval for B = 0.206 there is a decay factor of 4 and for B = 0.214 there is a decay factor of 60. Injun saw no marked change in flux as a result of a modest size magnetic storm.

The only decay process we understand well enough to calculate is coulomb scattering. Particle time histories have been calculated for coulomb scattering and characteristic times determined (Reference 5). The time to reach a scattering equilibrium (which is also about the time for this equilibrium to decay to 1/e intensity) for different L values is listed in Table 4. Welch, Kauffman, et al. (Reference 5) first calculated these for solar maximum atmospheric densities and now, assuming that the density is less by a factor of 10, we get the values in Table 4.

The air densities are not well known and the calculated times may be wrong by a factor of 5 or more. The calculated variation with L, however, should be fairly good. The Injun data show that the calculated times are of the right order of magnitude. The times show that the high flux region should last even through the next solar maximum if coulomb scattering is the principle loss process.

Table 4
Time Until Scattering Equilibrium for Different Values of L.

L	Calculated τ (days)	Measured τ
1.20	10	~1 month
1.25	150	–
1.30	1500	–
1.35	~3000	–
1.40	~10,000	–

REFERENCES

1. O'Brien, B. J., Laughlin, C. D., and Van Allen, J. A., "Geomagnetically Trapped Radiation Produced by a High-Altitude Nuclear Explosion on July 9, 1962," *Nature* 195(4845):939-943, September 8, 1962.

2. Marshall, J. S., and Ward, A. G., "Absorption Curves and Ranges for Homogeneous β-Rays," *Can. J. Res.* 15A, 39-41, March 1937.

3. McIlwain, C., "Coordinates for Mapping the Distribution of Magnetically Trapped Particles," *J. Geophy. Res.* 66(11):3681-3691, November 1961.

4. Rosenzweig, W., Gummel, H. K., and Smits, F. M., "Solar Cell Degradation Under 1 Mev Electron Bombardment," submitted to *J. Appl. Phys.*

5. Welch, J. A., Kauffman, R., et al., "Scattering Loss of Fission Beta Particles from High Altitude Explosions," Air Force Special Weapons Center Report 2-0038, August 1962.

Appendix A

Shielding and Radiation Doses

Included here for the sake of completeness are some crude calculations on shieldings and dosages.

One consideration that is important in some shielding calculations is bremsstrahlung. The doses delivered by the x-rays made by bremsstrahlung will be larger than the direct electron doses for large shield thicknesses.

The fraction of the energy of an electron that goes into bremsstrahlung may be calculated from:*

$$\frac{E_{brem}}{E_{ion}} = \frac{ZE^2}{1600} ,$$

where Z is the atomic number of the material involved. For the fission energy spectrum the average energy is about 1 Mev;

$$\frac{E_{brem}}{E_{ion}} = \begin{array}{cccc} C & Al & Fe & Pb \\ 0.004 & 0.008 & 0.015 & 0.050 \end{array}$$

The energy spectrum of the x rays will be something like that in Figure A1. There will be a very few x rays up to 8 Mev, but not many over 2 or 3 Mev. The low energy x rays (below about 100 kev) will be absorbed in the shielding. This will remove about half the total energy in the x rays. The resultant transmitted energy spectra will have a peak at about 1/2 Mev (Figure A1). The x rays transmitted through the shield will be quite penetrating. Their mean free path will be roughly 20 gms/cm². This means two things. First, they will be hard to absorb, and therefore it will take a lot more shielding to absorb them. Second, because they are hard to absorb, they will not be counted efficiently by a particle counter and also will result in less radiation dose.

We can now calculate crudely the counting efficiency of the Injun (1961 o2) 213 GM counter.

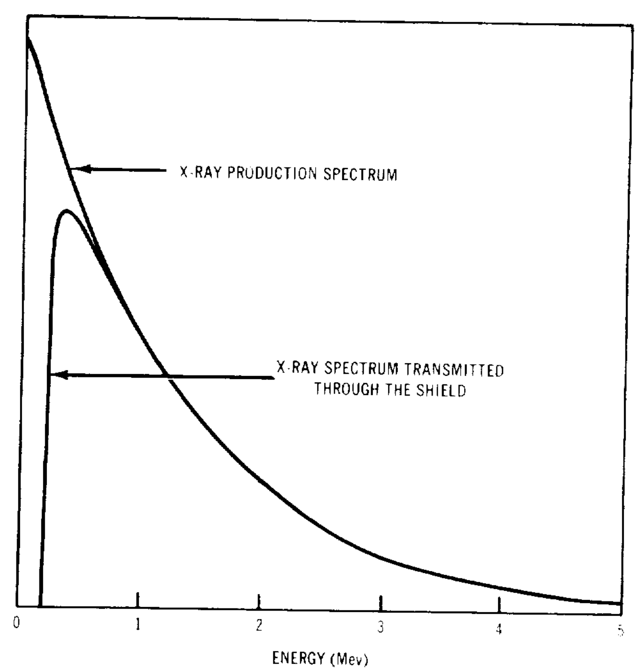

Figure A1—A crude bremsstrahlung x-ray energy spectrum.

*Fermi, E., "Nuclear Physics," A course given by Enrico Fermi at the University of Chicago, Notes compiled by Orear, J., Rosenfeld, A. H., and Schluter, R. A., University of Chicago Press, revised edition, 1950.

From Figure 9 of the body of this report we see that it would only count about 1/20,000 of the fission electrons directly. But we find that 0.05 of the energy is converted to bremsstrahlung, of which half is absorbed in the shield. The mean energy of these x rays will be about 1/2 Mev. A normal GM counter will detect these x rays with about 1 percent efficiency. This gives

$$(0.05)(0.01) = 1/2000 ,$$

for the fraction of the electrons counted via bremsstrahlung. This calculation is not very accurate but it does show that the Injun counter counts electrons via bremsstrahlung with about the observed efficiency.

Manned Flight

The effects of the new radiation belt on manned flights must be considered. For the Mercury project the total flux that would be encountered for a six orbit mission with the MA-7 (1962 τ1) orbit is 0.24×10^{10} electrons/cm^2 outside the vehicle, or 80 r (3×10^7 electrons/cm^2 = 1 r). The shielding of the vehicle is such that about 1 percent of this dose is delivered to the astronaut, about 1 r.

The mercury dose is almost all received in the South Atlantic "hot spot" (see Figure 8 of the body of the report) and occurs mainly on orbits 4, 5, and 6. The breakdown of the 1 r dose inside the capsule by orbits is given in Table A1.

Table A1
Radiation Dose per Orbit for a 6 Orbit Flight on the MA-7 Orbit.

Orbit	Dose (r)
1	0.003
2	0.01
3	0.03
4	0.1
5	0.3
6	0.6

NASA-Langley, 1963 G-337